

# SYNERGISTIC PERFORMANCE OF LOW-TEMPERATURE PLASMA ASSISTED THERMAL CO<sub>2</sub> METHANATION OVER Ni AND Co-BASED ZEOLITE CATALYSTS

Soipatta Soisuwan<sup>a</sup>, Patiparn Boonruam<sup>a</sup>, Piyachat Wattanachai<sup>a</sup>, Héctor Morillas<sup>b</sup>, Settakorn Upasen<sup>a\*</sup>

<sup>a</sup>Department of Chemical Engineering, Engineering Faculty, Burapha University, Chonburi, Thailand

<sup>b</sup>Department of Analytical Chemistry, Faculty of Science and Technology, University of the Basque Country (UPV/EHU), Bilbao, Basque Country, Spain

## Article history

Received

10 June 2025

Received in revised form

14 August 2025

Accepted

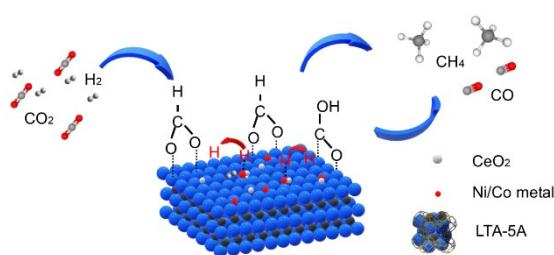
27 October 2025

Published online

31 May 2026

\*Corresponding author  
settakorn@eng.buu.ac.th

## Graphical abstract



## Abstract

Carbon capture utilization and storage (CCUS) is a crucial strategy platform for meeting net-zero emissions goals. In this research, the methanation reaction - carbon dioxide (CO<sub>2</sub>) waste gas converted into methane (CH<sub>4</sub>) fuel gas - was evaluated at elevated temperatures (200-400 °C) using a thermal catalytic (TC) process and at low temperatures (25-150 °C) using a plasma-assisted thermal catalytic (PTC) process. The dry-impregnation method was used to prepare catalysts in the formula of Ni-xCeO<sub>2</sub>/LTA-5A and Co-xCeO<sub>2</sub>/LTA-5A, where x is a CeO<sub>2</sub> promoter amount varied from 0-15 wt.%. It aims to seek its effect on catalytic activity and productivity. A constant 15 wt.% of Ni and Co active metals were mobilized on zeolite LTA-5A supporters. The advanced techniques i.e. SEM-EDX and BET chemisorption were performed to characterize the surface and bulk properties of all catalysts. In the TC process for all prepared catalysts, the temperature variable highly affected the CO<sub>2</sub> conversion and CH<sub>4</sub> selectivity - resulting in 94-99% CO<sub>2</sub> conversion and 93-95% CH<sub>4</sub> selectivity at 400 °C. An appropriate amount of 5 wt.% CeO<sub>2</sub> promoter could promote and stabilize the catalytic performance. The nickel-based metal catalyst showed a positive sign of CH<sub>4</sub> production at low-temperatures DBD plasma-assisted thermal catalytic (PTC) process.

**Keywords:** Ni, Co, CeO<sub>2</sub>, CO<sub>2</sub> methanation, DBD plasma

© 2026 Penerbit UTM Press. All rights reserved

## 1.0 INTRODUCTION

Global warming has been playing an essential role in our life. The leading causes are the emission of greenhouse gases mainly composed of CO<sub>2</sub>. For this reason, in several years, scientists and engineers have developed many valuable techniques for CO<sub>2</sub> management, including storage, utilization, and reduction [1-3]. The utilization of CO<sub>2</sub>, in this research, is of utmost interest by converting CO<sub>2</sub> into impact-value products such as CH<sub>4</sub>, C<sub>2</sub>H<sub>6</sub>, and CO. The CO<sub>2</sub> substrates converting into CH<sub>4</sub> is generally called CO<sub>2</sub> methanation, which operates at intermediate to high temperatures under an H<sub>2</sub> ambiance. The transition metals, including Ni [4], Co [5], Nb [6], etc have been discovered and used as the most effective catalysts. However, the up-to-date

development trend focuses on an operation at atmospheric pressure and temperature. This is owed to the strategic goal of many industries to pose a facilitated process establishment, minimal energy utilization, and less-to-zero environmental impacts.

Plasma technology manipulates the fourth state of matter by applying a high electric field to a gas, ionizing it into electrons, ions, radicals, and neutral molecules (uncharged molecules or radicals). This ionization facilitates unique chemical reactions in gas conversion processes, as the plasma environment contains energized species that drive reactions involving electrically neutral molecules. The different plasma types such as a thermal torch, plasma arc, and Dielectric Barrier Discharge (DBD) can be generated according to equipment, installation, and discharge

characteristics. In general, the plasma phenomenon occurs when sufficient energy proceeds through atoms or molecules, it creates an ionized gas, called free electrons. They will collide with the molecules of matter breaking the bonds between atoms, molecular disintegration, and possibly rearranging into another stable molecule [7]. For instance, in the CO<sub>2</sub> dissociation process using plasma, the OC=O bond is broken requiring only 5.5 eV of potential in the plasma source [8]. Farhan Ahmad and co-workers [9] performed the CO<sub>2</sub> methanation via plasma catalytic process at a temperature of 150–400°C using 10%Ni/Al<sub>2</sub>O<sub>3</sub> as tested catalysts. They reported that the CO<sub>2</sub> conversion was as high as 63%. The authors also described the synergy between the activated gas phase and the catalyst in the hybrid system. Plasma irradiation affects the physical-like properties of catalysts, i.e., increasing metal dispersion and particle size reduction, consequently enhancing a better methanation process. However, the catalyst type also plays an important role in the conversion and selectivity of the methanation process. The most widely active catalysts used for the plasma-catalytic process of CO<sub>2</sub> methanation are included in the VIII B metals group, for instance, Ni [10] and Co [11] coated on various porous supporters, i.e., activated carbon [12], aluminum oxide [13], ceria-zirconia [14]. Among the most studied systems, Co and Ni metal catalysts allowed considerable methanation rates with high selectivity and methane yield. The surface area and pore size of the supporter solid are vital parameters to enhance catalyst performance hydrogenation of carbon dioxide [15]. To improve the catalytic activity, metal oxide is commonly employed as a promoter material. Hezhi Liu [16] found that the appropriate amount of CeO<sub>2</sub> promoter significantly affected the interaction between the active metal and the supporter, consequently leading to improved catalytic performance.

This study investigates the influence of active metal species, namely nickel (Ni) and cobalt (Co), and the effect of cerium oxide (CeO<sub>2</sub>) promoters in the thermal catalytic (TC) methanation reaction. The catalysts were characterized for their physical properties, including morphology and specific surface area, using advanced analytical techniques such as scanning electron microscopy coupled with energy-dispersive X-ray spectroscopy (SEM-EDX) and Brunauer-Emmett-Teller (BET) surface area analysis. Additionally, the synergistic performance of a dielectric barrier discharge (DBD) plasma-assisted thermal catalytic (PTC) process was assessed in conjunction with the different catalyst formulations.

## 2.0 METHODOLOGY

### 2.1 Chemicals

All reagents used in this work are chemical reagent grade except the ethyl alcohol, which is lab-grade with a 99% assay. All chemicals were used as received without further purification or treatment.

### 2.2 Catalyst Synthesis

The catalyst preparation was done using a conventional dry impregnation method. The commercial zeolite LTA type 5A supplied by the Thai Silicate Chemicals company was used as a supporter, and CeO<sub>2</sub> was used as a promoter. First, the fresh

LTA-5A powder was thermally treated at 110°C for 6 hours using a vacuum oven. Then, the dried LTA-5A powder was impregnated with a selected Co and Ni active metal of 15 wt.%. The nickel and cobalt metals were received from Ni(NO<sub>3</sub>)<sub>2</sub>·6H<sub>2</sub>O and Co(NO<sub>3</sub>)<sub>2</sub>·6H<sub>2</sub>O precursors, respectively. The CeO<sub>2</sub> promoter was added with two levels of 0 and 5 wt.%. The target amount of metal and promoter were weighed and dissolved in pure ethanal 10 ml. Then, it was slowly dropped into 10-gram dried LTA-5A powder. The well-mixed precursor solid was dried at 80°C for 6 hours. Consequently, it was placed in an oven chamber performing a calcination process at 650°C and ambient pressure for 4 hours. Lastly, the calcined samples underwent a reduction step under an H<sub>2</sub> ambient at 450°C for 2 hours. Then, all prepared catalysts are denoted as Ni-xCeO<sub>2</sub>/LTA-5A and Co-xCeO<sub>2</sub>/LTA-5A, where x represents the mass percentage of the CeO<sub>2</sub> promoter.

### 2.3 Catalyst Characterization

The surface morphology and particle size distribution of Ni/LTA-5A, Ni-5CeO<sub>2</sub>/LTA-5A, Co/LTA-5A, and Co-5CeO<sub>2</sub>/LTA-5A were characterized using the SEM method JEOL JSM-6400 Scanning Electron Microscope. In addition, the elemental quantitative of active metals on the surface catalyst was determined via energy-dispersive X-ray spectroscopy (EDX). The specific surface area and porosity catalysts were analyzed by the N<sub>2</sub> adsorption-desorption isotherm method using an instrument of Quantachrome NOVA-3000 system at 77 K.

### 2.4 CO<sub>2</sub> Methanation Testing

The catalytic activity towards CO<sub>2</sub> methanation reaction under two different processes, conventional thermal-catalytic (TC) and plasma-assisted thermal-catalytic (PTC) processes was studied. The thermal-catalytic process was installed with a traditional heating chamber. The TC test was operated at a temperature range of 100–400°C while the PTC process underwent a low temperature of 30–200°C. [Note: the PTC process was not able to run at high temperatures because of the thermal resistant limitation of the plasma instrument] As shown in Figure 1, the experimental setup consists of mass flow controllers, a high-voltage power generator, low-voltage (LV) and high-voltage (HV) electrodes, a conventional heating oven, a fixed-bed tube reactor, and a saturator unit. The TC reactor used a stainless-steel tube with 0.6 cm outside diameter and 21 cm in length. The PTC reactor was made of a quartz tube with ~15 mm outside diameter and 1.2 mm thickness. The HV electrode of a 2.5 mm-concentric stainless-steel rod was placed inside the reactor, and the LV electrode of the aluminum wire rod was wrapped with an effective length of 10 cm around the quartz tube. The catalyst loading of 500 mg was packed into the TC or PTC reactor for each testing run.

The gas stream comprises 30% carbon dioxide (CO<sub>2</sub>) by volume, with nitrogen (N<sub>2</sub>) constituting the remaining 70%. The total volumetric flow rate of the mixture is 16 mL/min. The limiting reactant of H<sub>2</sub> gas was set at 4-fold to one mole of CO<sub>2</sub> input; hence the H<sub>2</sub> flow rate was about 28 ml/min. The mixed gas stream was continuously flowing for at least 5 minutes. Then, the heating oven was set at the required testing temperature (with or without the active plasma laser of 15 kV). The outlet gas stream first flowed through the saturator tube to capture moisture as a by-product of methanation. Keep the

reaction running for ten minutes, then, the gas sample was automatically injected into the gas chromatography equipped with a thermal conductivity detector (He as the carrier gas) and a flame ionization detector (H<sub>2</sub> as the carrier gas). Seven to ten repetitions of injections with an interval time of 10 minutes were performed. The characteristics of GC chromatographs were further interpreted as regards the composition of the gas mixture, and the CO<sub>2</sub> conversion, product yield as well as productivity rate were calculated as the following equation:

$$\text{CO}_2 \text{ conversion (\%)} = \frac{\text{CO}_2 \text{ converted (mol/s)}}{\text{CO}_2 \text{ input (mol/s)}} \times 100 \quad (1)$$

$$\text{CH}_4 \text{ selectivity (\%)} = \frac{\text{CH}_4 \text{ produced (mol/s)}}{\text{CO}_2 \text{ converted (mol/s)}} \times 100 \quad (2)$$

$$\text{CH}_4 \text{ yield (\%)} = \frac{\text{CH}_4 \text{ produced (mol/s)}}{\text{CO}_2 \text{ input (mol/s)}} \times 100 \quad (3)$$

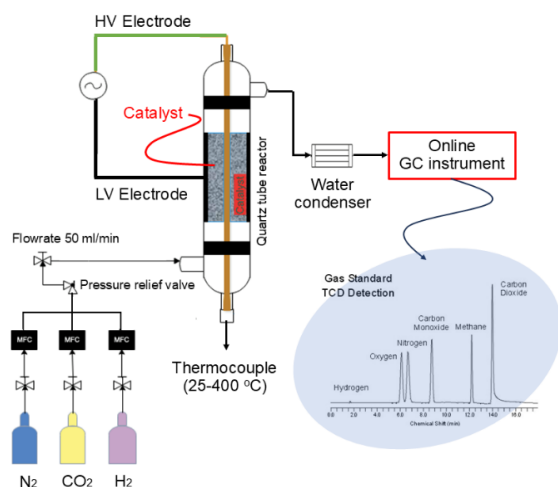


**Figure 1** Schematic diagram of methanation experimental apparatus using the thermal catalytic (TC) and plasma-thermal catalytic (PTC) process

### 3.0 RESULTS AND DISCUSSION

#### 3.1 Physical Characteristics Of Catalysts

The morphology of all prepared catalysts was analyzed by SEM-EDX techniques. Representative micrograph images and basic x-ray patterns for Ni/LTA-5 and Ni-5CeO<sub>2</sub>/LTA-5 samples are shown in Figure 2. It is observed that the LTA-5 supporter had a clear lattice fringe of cubic shape. The average LTA-5 particle size was shown at  $1.89 \pm 0.13 \mu\text{m}$ . Active metal particles for both bare Ni/LTA-5 (Figure 2-a1) and Co/LTA-5 (Figure 2-b1) catalysts were well dispersed on the LTA-5 surfaces. However, the Co/LTA-5 sample showed a smaller grain size ( $0.153 \pm 0.07 \mu\text{m}$ ) and a lower aggregation degree than the Ni particle sample ( $0.298 \pm 0.05 \mu\text{m}$ ). In addition, an increasing number of fine particles were obtained for Ni-5CeO<sub>2</sub>/LTA-5 sample (Figure 2-a2, a3) and Co-5CeO<sub>2</sub>/LTA-5 sample (Figure 2-b2, b3), consequently giving rise for particle agglomeration. This was affected by the addition of 5 wt.% CeO<sub>2</sub> content. According to the EDX analysis, the Ni active element for the Ni-5CeO<sub>2</sub>/LTA-5 sample was detected by 49.9 wt.% and a Ce element in the form of CeO<sub>2</sub> promoter was 14.5 wt.%. For the Co-5CeO<sub>2</sub>/LTA-5 sample (Figure

2-b3), the Co-active metal was shown at 43.2 wt.% and a Ce element was 11.7 wt.%. The elemental analysis result was truly confirmed to the weight ratio of active species (Ni, Ce) per CeO<sub>2</sub> promoter as 1:0.3.

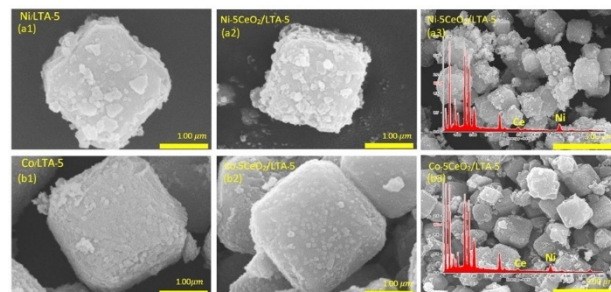


**Figure 2** Representative SEM images and EDX patterns for prepared catalysts: (a1–a3) Ni-based/LTA-5 and (b1–b3) Co-based/LTA-5

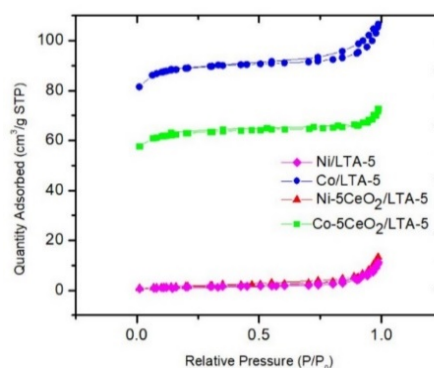


**Figure 3** Brunauer–Emmet–Teller (BET) analysis of prepared catalysts (Ni/LTA-5, Co/LTA-5, Ni-5CeO<sub>2</sub>/LTA-5 and Co-5CeO<sub>2</sub>/LTA-5): N<sub>2</sub> adsorption and desorption isotherm as a function of P/P<sub>0</sub>

The N<sub>2</sub> adsorption isotherm curves (Figure 3) for all catalyst samples were received by the Brunauer–Emmett–Teller (BET) technique. The Ni-based catalyst sample exhibited a physisorption isotherm Type III – the hysteresis loop (P/P<sub>0</sub>) of N<sub>2</sub> adsorption and desorption greater than 0.8. For the Co-based catalysts, the isotherm curves showed two regions of the P/P<sub>0</sub> < 0.2 and P/P<sub>0</sub> > 0.8 hysteresis loop. According to the IUPAC classification [17], the first hysteresis loop (P/P<sub>0</sub> < 0.2) was identified as Type I, and the second one (P/P<sub>0</sub> > 0.8) was a Type III hysteresis loop. Moreover, these various hysteresis loop behaviors indicated characteristics of microporous (a pore size greater than 50 nm) and/or mesoporous material (a pore size of 2–50 nm). Table 1 displays an estimated surface area, pore volume, and pore size for prepared Ni-based/LTA-5 and Co-based/LTA-5 catalysts with 0–5 wt.% of CeO<sub>2</sub> content. The measured BET surface area of Co-based catalysts was larger than that of Ni-based catalysts. The surface area of Co-xCeO<sub>2</sub>/LTA-5 catalysts decreased because of the addition of CeO<sub>2</sub> content from 297.79 m<sup>2</sup>/g for Co/LTA-5 to 210.6474 m<sup>2</sup>/g for Co-5CeO<sub>2</sub>/LTA-5, corresponds to the decrease of the pore volume from 0.1650 to 0.110 cm<sup>3</sup>/g. The Ni-xCeO<sub>2</sub>/LTA-5 catalyst had a similar trend result - adding the amount of 5 wt.% CeO<sub>2</sub> led to a decrease in the surface area. The reduction in surface area with 5 wt.% CeO<sub>2</sub> arises from particle sintering and crystallite growth, leading to decreased porosity and surface availability.

**Table 1** Estimated surface area, pore volume, and pore size for all prepared catalysts

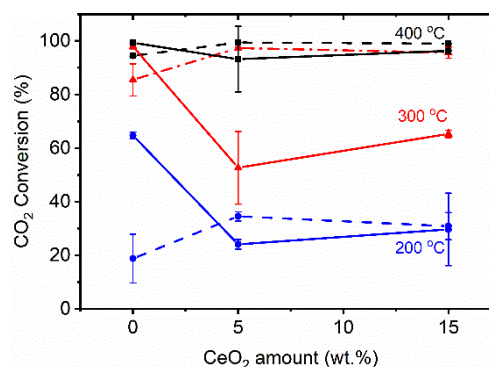
Sample	Surface area (m <sup>2</sup> /g)	pore size (nm)	pore volume (cm <sup>3</sup> /g)
Ni/LTA-5	6.54	11.00	0.0152
Ni-5CeO <sub>2</sub> /LTA-5	5.52	10.77	0.0175
Co/LTA-5	297.80	2.20	0.1650
Co-5CeO <sub>2</sub> /LTA-5	210.65	2.08	0.1100

### 3.2 Thermal Catalytic (TC) Testing

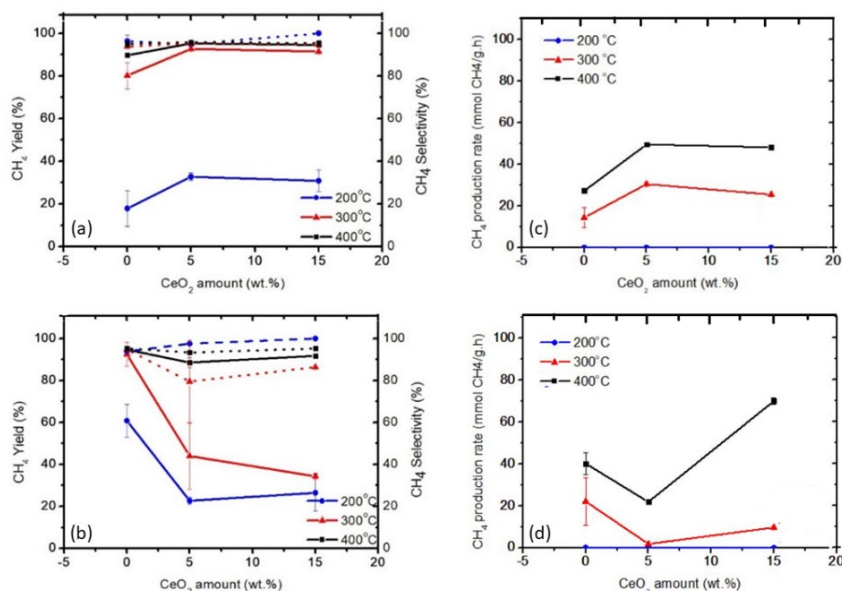
#### 3.2.1 Active Metals and CeO<sub>2</sub> Promoter

Nickel and cobalt metals take the initiative in catalytic active sites. The case of non-CeO<sub>2</sub> doping (Ni/LTA-5 and Co/LTA-5) samples gave significantly different results on CO<sub>2</sub> methanation. The Co metal tended to show higher activity and productivity than Ni metal, for example, operating at 300 °C, the Co/LTA-5 catalyst gave 98% CO<sub>2</sub> conversion (Figure 4, solid line), while the Ni/LTA-5 catalyst gave only 86% CO<sub>2</sub> conversion (Figure 4, dashed line). The obtained CH<sub>4</sub> production rates were 22.7 mmol CH<sub>4</sub>/g-h and 14.38 mmol CH<sub>4</sub>/g-h for Ni-based (Figure 5c) and Co-based catalysts (Figure 5d). Both types of metal active sites showed an insignificant effect on the CH<sub>4</sub> selectivity values. In contrast, the activity and productivity of the methanation reaction for nickel-based catalysts were higher than those of Co-based catalysts when incorporated with the CeO<sub>2</sub> promoter, as explained in the following paragraph. The effect of the CeO<sub>2</sub> promoter is attributed to the formation of the side product carbon monoxide via the reverse water-gas shift reaction [18].

The CO<sub>2</sub> methanation was performed over the Ni-xCeO<sub>2</sub>/LTA-5 and Co-xCeO<sub>2</sub>/LTA-5 catalysts with CeO<sub>2</sub> content varying from 0 to 15 wt.%. For the Ni-based catalyst (Figure 4, dash),

**Figure 4** CeO<sub>2</sub> amount effect on % CO<sub>2</sub> conversion for TC methanation: (dashed-line) Ni-based (solid-line) Co-based catalyst

incorporating a CeO<sub>2</sub> promoter enhanced a better CO<sub>2</sub> conversion. Adding 5 wt.% CeO<sub>2</sub> and 15 wt.% CeO<sub>2</sub> into yielded 35% and 31% CO<sub>2</sub> conversion, respectively. It is because the addition of the CeO<sub>2</sub> promoter improved and stabilized the catalytic performance more effectively [16]. However, an excessive amount of CeO<sub>2</sub> significantly led to reduced CO<sub>2</sub> conversion due to the reduction of the catalyst surface. The high catalyst surface gives high catalytic activity [19]. In addition, it has been reported that the excess promoters might cover the active metal particles on the catalyst surface, consequently resulting in a slowdown of the reaction activity. However, it shows contrasting observations for the Co-based catalyst (Figure 4, solid line). The virgin Co/LTA-5 catalyst gave better CO<sub>2</sub> conversion compared to the Co-5CeO<sub>2</sub>/LTA-5 and Co-15CeO<sub>2</sub>/LTA-5 catalysts. This implies that CeO<sub>2</sub> could not promote reaction activity on a Co-based catalyst.

**Figure 5** Effect of CeO<sub>2</sub> promoter amount on yield (solid) and CH<sub>4</sub> selectivity (dashed) for (a) Ni-based and (b) Co-based catalysts; and CH<sub>4</sub> production rate (mmol CH<sub>4</sub>/g-h) for (c) Ni-based and (d) Co-based catalysts

The percentage of CH<sub>4</sub> selectivity for Ni-based/LTA-5 catalyst (Figure 5a) was not significantly affected by the amount of CeO<sub>2</sub> promoter. It exhibited almost the same value for every CeO<sub>2</sub> dosage. However, adding CeO<sub>2</sub> into the Ni-based/LTA-5 catalyst enhanced the CH<sub>4</sub> yield as well as the CH<sub>4</sub> production rate, for instance, the Ni-5CeO<sub>2</sub>/LTA-5 catalyst resulted in almost 100% CH<sub>4</sub> yield and 50 mmol CH<sub>4</sub>.g<sup>-1</sup>.h<sup>-1</sup>. The CeO<sub>2</sub> promoter was found to stabilize the nickel species more effectively [20]. Hezhi Liu and co-workers [16] also discovered that catalysts with CeO<sub>2</sub> exhibited high catalytic performance for higher hydrocarbon reforming. For the Co-based catalyst, illustrated in Figure 5b, the CeO<sub>2</sub> promoter tends to lower the CH<sub>4</sub> yield corresponding to the lower activity of CO<sub>2</sub> methanation as discussed above. Moreover, it influenced a lower selectivity of CH<sub>4</sub> products and was more favorable to carbon monoxide formation. The CH<sub>4</sub> production rate (Figure 5d) was uncertain - it might be because the CeO<sub>2</sub> influences less stable Co-active species than nickel species. However, the proportion of 1:1 by wt.% CeO<sub>2</sub> to Co metal, yielded the highest CH<sub>4</sub> production rate of 70 mmol CH<sub>4</sub>/g.h operating at 400°C.

### 3.2.2 Temperature Effect

The influence of reaction temperature (100-400 °C) on the CO<sub>2</sub> conversion is illustrated in Figure 6. The CO<sub>2</sub> conversion for all prepared catalysts operated at 100°C was null. However, it increased rapidly when the temperature was above 100°C. At low-temperature range (below 200°C), the CO<sub>2</sub> conversion of CO<sub>2</sub> for the Co-based catalyst, especially bare Co/LTA-5 (64% CO<sub>2</sub> conversion), was higher than that for the Ni-based catalyst (19-35% CO<sub>2</sub> conversion), with similar result compared to with the research of Zuzeng Qin and co-workers [21]. For intermediate temperature (200-400 °C), CO<sub>2</sub> conversion for Ni-based catalysts rapidly increased and reached about 80-95% at 300°C. For the Co-based catalyst, only the bare Co/LTA-5 catalyst gave nearly

98% CO<sub>2</sub> conversion at a similar temperature. All tested catalysts showed 100% CO<sub>2</sub> conversion at 400 °C. Kristian Stangland and co-workers [20] also revealed that the methanation reaction of CO<sub>2</sub> is more preferable at intermediate temperatures (less than 500°C), where the %CO<sub>2</sub> conversion reached close to 100%. The higher the temperature was, the higher the reaction activity occurred [19].

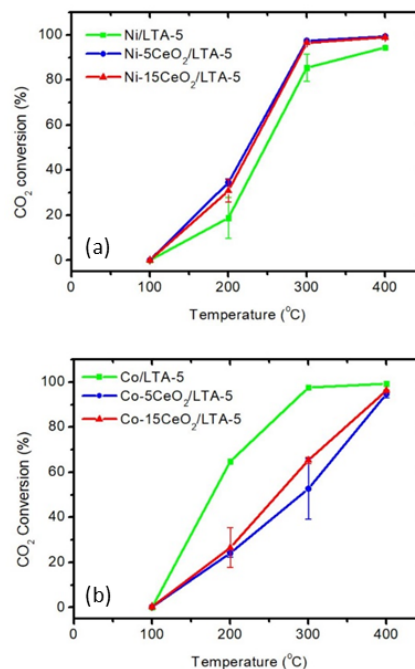


**Figure 6** Temperature effect on %CO<sub>2</sub> conversion for TC methanation process: (a) Ni-based (b) Co-based catalyst

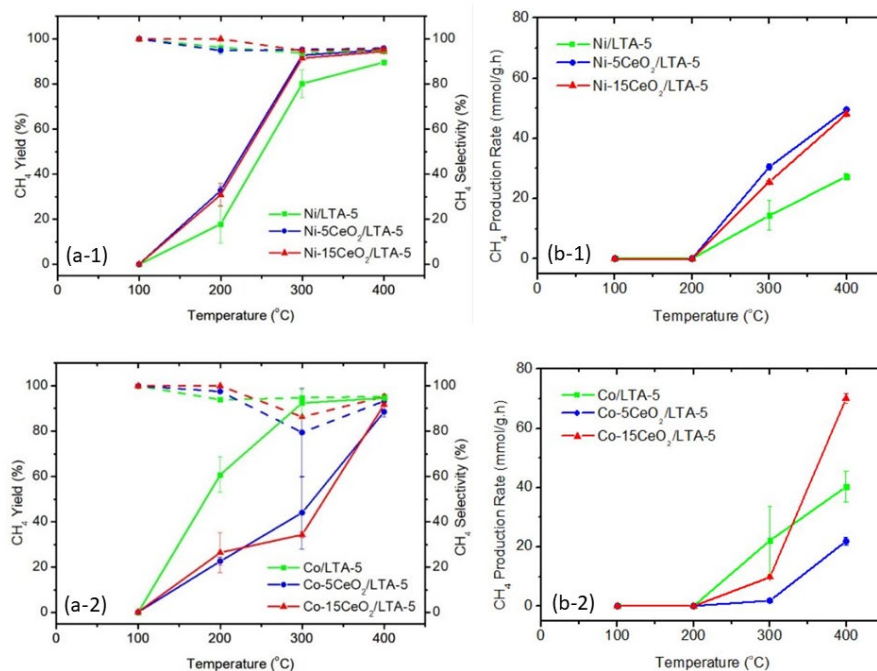


**Figure 7** (a-1, a-2) CH<sub>4</sub> yield and selectivity profile (b-1, b-2) productivity rate (mmol CH<sub>4</sub>/g.h) in various operating temperatures

The trend of %CH<sub>4</sub> yield versus operating temperature for Ni-based/LTA-5 catalyst (Figure 7 a-1) and Co-based/LTA-5 catalyst (Figure 7 a-2) remarked that the CH<sub>4</sub> yield increased with increasing temperature. Interestingly, operating temperature of 200°C, the methanation reaction employing a Co/LTA-5 catalyst resulted in a 2-fold yield percentage higher than that of using a Ni/LTA-5 catalyst. When the temperature reached 300°C, the highest CH<sub>4</sub> yield resulted in about 80 – 90% for both operating Ni/LTA-5 and Co/LTA-5 series. However, adding CeO<sub>2</sub> promoter into Co/LTA-5 significantly affected the yield of CH<sub>4</sub> product – favorable temperature for methanation reaction was shifted higher as 400°C. Operating at high temperatures, however, the reverse water gas shift response was also favored [20] - led to produce carbon monoxide (CO) gas as a side product.

The CH<sub>4</sub> selectivity results for Ni-based/LTA-5 (Figure 7 a-1) and Co-based/LTA-5 catalysts (Figure 7 a-2) are presented in the dashed line. The methanation reaction for all catalysts was highly selective at low temperatures (below 200°C). When the elevated temperature was above 200°C, the CH<sub>4</sub> selectivity was slightly decreased and occurred in a higher %CO selectivity from reverse water gas shift reaction. For all proportions of Ni-CeO<sub>2</sub> catalysts, %CO selectivity was found 4-7% approximately, and there was no significant difference in the number of CO selectivity at 200-400°C. In contrast, the Co/LTA-5 catalyst, especially the catalyst doped CeO<sub>2</sub>, was remarkably found in low CH<sub>4</sub> selectivity (80-85%) at 300 °C. At this point, the CO product was selective about 17-21%. The trend of methane production rate (mmol/ g. h) in the function of temperatures behaved correspondingly to the CH<sub>4</sub> yield. It resulted as high as 49.5 mmol/g.h for Ni-based/LTA-5 (Figure 7 b-1) and 70 mmol/g.h for Co-based/ LTA- 5 catalyst (Figure 7 b-2) at an operating temperature of 400°C. However, the number of CH<sub>4</sub> product rates varied depending on the CeO<sub>2</sub> content, which was discussed earlier.

### 3.3 Plasma-Assisted Thermal-Catalytic (PTC) Testing

In brief review, several factors influence the mechanism of plasma throughout the methanation reaction, i.e. dielectric materials, voltage, discharge gap, temperature, etc. Mora and co-workers [18] reported that different dielectric materials show different relative dielectric permittivity coefficient values. The CO<sub>2</sub> hydrogenation under DBD plasma technology using alumina material as the dielectric barrier was better than quartz because the alumina has a greater relative dielectric permittivity coefficient. Regarding the voltage effect, a high voltage value results in a high CH<sub>4</sub> selectivity due to a large plasma density [8]. A small discharge gap between the two electrodes rises in input power density, which causes enhancement in the electric field, consequently, resulting in a constructive on the CO<sub>2</sub> conversion and CH<sub>4</sub> selectivity. Magdalena Nizio and co-workers [22] show the effect of temperature on plasma-catalytic methanation over Ni-Ce-Zr hydrotalcite-derived catalysts. When using DBD plasma in the temperature range of 0-450°C, CO<sub>2</sub> conversion rose at lower temperatures – the temperature of 120°C onwards. In contrast to the reaction when performed under a catalyst alone - the CO<sub>2</sub> modification enhanced at higher temperatures at 320°C. Parameters and catalytic performance results of both TC and TPC processes for the CO<sub>2</sub> methanation reaction are included in Table 2.

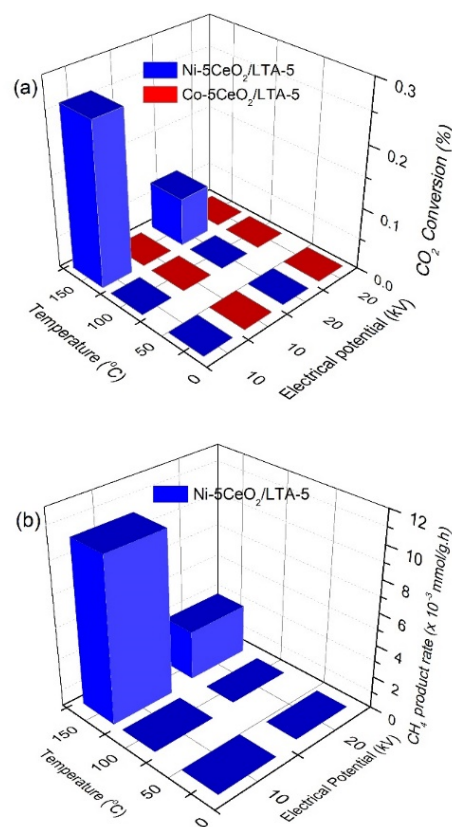


**Figure 8** (a) CO<sub>2</sub> conversion and (b) CH<sub>4</sub> production rate of thermal-plasma catalytic testing for methanation reaction using Ni-5CeO<sub>2</sub>/LTA-5 and Co-5CeO<sub>2</sub>/LTA-5 catalyst

In this research, the possibility of the DBD plasma assisted with the thermal catalytic process was sought to lower the reaction temperature. The thermal catalytic process was tested in the temperature range of 25 – 150°C. Two catalyst types of Co-5CeO<sub>2</sub>/LTA-5 and Ni-5CeO<sub>2</sub>/LTA-5, which resulted as the most active catalysts at the low temperature shown in the previous section, were selected. The results show that the Co-5CeO<sub>2</sub>/LTA-5 sample (Figure 8a) was inactive under DBD plasma of 10kV and 20 kV at all investigated temperatures – giving close to zero percent of CO<sub>2</sub> conversion. Regarding Yan Sin's observation [23], the test of cobalt particles as an active catalyst at the utmost high pressure and temperature via glow discharge plasma type devoted a favorable reaction to the fisher-tropsch. It produced the main product of C<sub>5-12</sub> and only a few CH<sub>4</sub> selective. In the case of the Ni-5CeO<sub>2</sub>/LTA-5 sample, the methanation reaction has a high potential to undergo at above 150 °C even if it resulted in very low CO<sub>2</sub> conversion. However, an excess electrical voltage (20 kV) of the TPC process decreased the activity and productivity of the methanation reaction – lowering almost 2-fold of %CO<sub>2</sub> conversion. The observation of CH<sub>4</sub> production rate was 3-10 x 10<sup>-3</sup> mmol/g.h (Figure 8b), applying an electrical voltage of 10 kV resulted in a quadruple higher CO<sub>2</sub> conversion than a 20 kV electrical voltage.

Table 2 Summary of Ni-based catalyst and Co-based catalyst for the methanation reaction

Catalyst	Method	Conditions			CO <sub>2</sub> Conversion (%)	CH <sub>4</sub> selectivity (%)	Ref.
		Temp. (°C)	Gas Feed <sup>a</sup>	Potential/Pressure			
Co/LTA-5	Thermal Cat.	200-400	4:1, 51	1 atm	99	95	This study
Co-5CeO <sub>2</sub> /LTA-5			4:1, 51	1 atm	94	93	
Co-15CeO <sub>2</sub> /LTA-5			4:1, 51	1 atm	96	95	
Ni/LTA-5	Thermal Cat.	200-400	4:1, 51	1 atm	94	98	This study
Ni-5CeO <sub>2</sub> /LTA-5			4:1, 51	1 atm	99	95	
Ni-15CeO <sub>2</sub> /LTA-5			4:1, 51	1 atm	99	95	
5Ni/Al <sub>2</sub> O <sub>3</sub>	Thermal Cat.	150-400	4:1,150	1 atm	71	99	[24]
10Ni/Al <sub>2</sub> O <sub>3</sub>					74	99	
15Ni/Al <sub>2</sub> O <sub>3</sub>					75	99	
Ni-20CeO <sub>2</sub> /MCM-41	Thermal Cat.	250-450	4:1, 9,000*	1 atm	85.6	99.8	[25]
13Co <sub>2</sub> C/Al <sub>2</sub> O <sub>3</sub>	Thermal Cat.	350	4:1, 10,573*	11 atm	89	99	[26]
Ni-CeO <sub>2</sub> /LTA-5	DBD plasma	150	4:1, 51	10-20 kV.	0.2-0.4	100	This study
5Ni/Al <sub>2</sub> O <sub>3</sub>	DBD plasma	200-350	4:1,50	4-15 kV.		50	
10Ni/Al <sub>2</sub> O <sub>3</sub>					60	100	
15Ni/Al <sub>2</sub> O <sub>3</sub>					50	100	
5Co/CeZrO <sub>4</sub>	DBD plasma	150	4:1, 25	20 kV.	70	99	[27]

#### 4.0 CONCLUSION

This study clearly demonstrates that low-temperature dielectric barrier discharge (DBD) plasma-assisted thermal catalytic (PTC) processes are a promising, energy-efficient approach for converting CO<sub>2</sub> into methane. The plasma thermal-catalytic (PTC) process was able to essentially operate the CO<sub>2</sub> methanation process at a low temperature range (25-150 °C), specifically, performing at a temperature of 150 °C and an electrical potential of 10 kV using Ni-5CeO<sub>2</sub>/catalysts. The research also confirms that Ni and Co-based catalysts supported on zeolite LTA-5A, particularly those promoted with an optimal 5 wt.% CeO<sub>2</sub> influences a well-dispersed active metal, significantly enhances catalytic activity and selectivity toward methane production under a conventional thermal catalytic (TC) process at elevated temperatures (200-400 °C). Overall, integrating plasma with optimized energy density, catalyst types, or reactor design offers a practical and sustainable approach to greenhouse gas valorization, advancing carbon capture, utilization, and storage (CCUS) technologies towards carbon neutrality and environmental protection.

#### Acknowledgement

The authors gratefully acknowledge financial support from the National Research Council of Thailand provided to Burapha University under Grant No. 136/2564.

#### Conflicts of Interest

The author(s) declare(s) that there is no conflict of interest regarding the publication of this paper

#### References

[1] Song, C. 2006. Global challenges and strategies for control, conversion and utilization of CO<sub>2</sub> for sustainable development involving energy, catalysis, adsorption and chemical processing. *Catalysis Today*. 115(1): 2-32. DOI : <https://doi.org/10.1016/j.cattod.2006.02.029>

[2] Olah, G. A., Goepfert, A., & Prakash, G. K. S. 2009. Chemical Recycling of Carbon Dioxide to Methanol and Dimethyl Ether: From Greenhouse Gas to Renewable, Environmentally Carbon Neutral Fuels and Synthetic Hydrocarbons. *The Journal of Organic Chemistry*, 74(2): 487-498. DOI : <https://doi.org/10.1021/jo801260f>

[3] Le Quéré, C., Jackson, R. B., Jones, M. W., Smith, A. J. P., Abernethy, S., Andrew, R. M., . . . Peters, G. P. 2020. Temporary reduction in daily global CO<sub>2</sub> emissions during the COVID-19 forced confinement. *Nature Climate Change*. 10(7): 647-653. DOI : <https://doi.org/10.1038/s41558-020-0797-x>

[4] Upasen, S., Sarunchot, G., Srira-ngam, N., Poo-arporn, Y., Wattanachai, P., Praserttham, P., . . . Soisuwan, S. 2022. What if zeolite LTA4A and zeolite LTA5A used as Nickel catalyst supports for recycling carbon dioxide to green fuel methane. *Journal of CO<sub>2</sub> Utilization*. 55: 101803. DOI : <https://doi.org/10.1016/j.jcou.2021.101803>

[5] Li, J., Mei, X., Zhang, L., Yu, Z., Liu, Q., Wei, T., . . . Hu, X. 2020. A comparative study of catalytic behaviors of Mn, Fe, Co, Ni, Cu and Zn-Based catalysts in steam reforming of methanol, acetic acid and acetone. *International Journal of Hydrogen Energy*. 45(6): 3815-3832. DOI : <https://doi.org/10.1016/j.ijhydene.2019.03.269>

[6] da Silva, G. T. S. T., Nogueira, A. E., Oliveira, J. A., Torres, J. A., Lopes, O. F., & Ribeiro, C. 2019. Acidic surface niobium pentoxide is catalytic active for CO<sub>2</sub> photoreduction. *Applied Catalysis B: Environmental*. 242: 349-357. DOI : <https://doi.org/10.1016/j.apcatb.2018.10.017>

[7] Isayama, S., Shinohara, S., & Hada, T. 2018. Review of Helicon High-Density Plasma: Production Mechanism and Plasma/Wave Characteristics. *Plasma and Fusion Research*. 13: 1101014-1101014. DOI : <https://doi.org/10.1585/pfr.13.1101014>

[8] Ashford, B., Wang, Y., Wang, L., & Tu, X. 2019. Plasma-Catalytic Conversion of Carbon Dioxide. In X. Tu, J. C. Whitehead, & T. Nozaki (Eds.), *Plasma Catalysis: Fundamentals and Applications*. 271-307. Cham: Springer International Publishing

[9] Ahmad, F., Lovell, E. C., Masood, H., Cullen, P. J., Ostrikov, K. K., Scott, J. A., & Amal, R. 2020. Low-Temperature CO<sub>2</sub> Methanation: Synergistic Effects in Plasma-Ni Hybrid Catalytic System. *ACS Sustainable Chemistry & Engineering*. 8(4): 1888-1898. DOI : <https://doi.org/10.1021/acssuschemeng.9b06180>

[10] Danaci, S., Protasova, L., Lefevre, J., Bedel, L., Guilet, R., & Marty, P. 2016. Efficient CO<sub>2</sub> methanation over Ni/Al<sub>2</sub>O<sub>3</sub> coated structured catalysts. *Catalysis Today*. 273: 234-243. DOI: <https://doi.org/10.1016/j.cattod.2016.04.019>

[11] Li, W., Liu, Y., Mu, M., Ding, F., Liu, Z., Guo, X., & Song, C. 2019. Organic acid-assisted preparation of highly dispersed Co/ZrO<sub>2</sub> catalysts with superior activity for CO<sub>2</sub> methanation. *Applied Catalysis B: Environmental*. 254: 531-540. DOI: <https://doi.org/10.1016/j.apcatb.2019.05.028>

[12] Swalus, C., Jacquemin, M., Poleunis, C., Bertrand, P., & Ruiz, P. 2012. CO<sub>2</sub> methanation on Rh/γ-Al<sub>2</sub>O<sub>3</sub> catalyst at low temperature: "In situ" supply of hydrogen by Ni/activated carbon catalyst. *Applied Catalysis B: Environmental*. 125: 41-50. DOI: <https://doi.org/10.1016/j.apcatb.2012.05.019>

[13] Zhao, K. C., Li, Z. H., & Bian, L. 2016. CO<sub>2</sub> methanation and co-methanation of CO and CO<sub>2</sub> over Mn-promoted Ni/Al<sub>2</sub>O<sub>3</sub> catalysts.

- Frontiers of Chemical Science and Engineering*. 10(2): 273-280. DOI : <https://doi.org/10.1007/s11705-016-1563-5>
- [14] Nizio, M., Albarazi, A., Cavadias, S., Amouroux, J., Galvez, M. E., & Da Costa, P. 2016. Hybrid plasma-catalytic methanation of CO<sub>2</sub> at low temperature over ceria zirconia supported Ni catalysts. *International Journal of Hydrogen Energy*. 41(27): 11584-11592. DOI: <https://doi.org/10.1016/j.ijhydene.2016.02.020>
- [15] Shuwa, S. M., Jibril, B. Y., & Al-Hajri, R. S. 2018. Hydrogenation of toluene on Ni-Co-Mo supported zeolite catalysts. *Nigerian Journal of Technology*. 36: 1114-1123. DOI: <https://doi.org/10.4314/njt.v36i4.17>
- [16] Liu, H., Zou, X., Wang, X., Lu, X., & Ding, W. 2012. Effect of CeO<sub>2</sub> addition on Ni/Al<sub>2</sub>O<sub>3</sub> catalysts for methanation of carbon dioxide with hydrogen. *Journal of Natural Gas Chemistry*. 21(6): 703-707. DOI : [https://doi.org/10.1016/S1003-9953\(11\)60422-2](https://doi.org/10.1016/S1003-9953(11)60422-2)
- [17] Chen, X., & Zhang, Q. 2019. Recent advances in mesoporous metal-organic frameworks. *Particuology*. 45: 20-34. DOI: <https://doi.org/10.1016/j.partic.2018.09.007>
- [18] Mora, E. Y., Sarmiento, A., & Vera, E. 2016. Alumina and quartz as dielectrics in a dielectric barrier discharges DBD system for CO<sub>2</sub> hydrogenation. *Journal of Physics: Conference Series*. 687(1): 012020. DOI : <https://doi.org/10.1088/1742-6596/687/1/012020>
- [19] Wang, X., Zhen, T., & Yu, C. 2016. Application of Ni–Al-hydrotalcite-derived catalyst modified with Fe or Mg in CO<sub>2</sub> methanation. *Applied Petrochemical Research*. 6(3): 217-223. DOI: <https://doi.org/10.1007/s13203-016-0154-1>
- [20] Stangeland, K., Kalai, D., Li, H., & Yu, Z. 2017. CO<sub>2</sub> Methanation: The Effect of Catalysts and Reaction Conditions. *Energy Procedia*. 105: 2022-2027. DOI : <https://doi.org/10.1016/j.egypro.2017.03.577>
- [21] Ji, H., Qin, Z., Zhou, Y., Liu, Z., & Jiang, Y. 2017. Recent Advances in Heterogeneous Catalytic Hydrogenation of CO<sub>2</sub> to Methane. In M. Takht Ravanchi (Ed.), *New Advances in Hydrogenation Processes - Fundamentals and Applications*. Rijeka: IntechOpen
- [22] Nizio, M., Benrabbah, R., Krzak, M., Debek, R., Motak, M., Cavadias, S., . . . Da Costa, P. 2016. Low temperature hybrid plasma-catalytic methanation over Ni-Ce-Zr hydrotalcite-derived catalysts. *Catalysis Communications*. 83: 14-17. DOI: <https://doi.org/10.1016/j.catcom.2016.04.023>
- [23] Jin, Y., Xiao, G., Han, Y., Sun, F., Zhang, D., Zhang, Y., Li, J., & Hong, J. 2019. Products selectivity and reaction stability of cobalt-based Fischer-Tropsch catalysts affected by glow discharge plasma treatment and silica structure. *Catalysis Today*. 337: 139-146. DOI : <https://doi.org/10.1016/j.cattod.2019.04.023>
- [24] Biset-Peiró, M., Guilera, J., Zhang, T., Arbiol, J., & Andreu, T. 2019. On the role of ceria in Ni-Al<sub>2</sub>O<sub>3</sub> catalyst for CO<sub>2</sub> plasma methanation. *Applied Catalysis A: General*. 575: 223-229. DOI : <https://doi.org/10.1016/j.apcata.2019.02.028>
- [25] Wang, X., Zhu, L., Liu, Y., & Wang, S. 2018. CO<sub>2</sub> methanation on the catalyst of Ni/MCM-41 promoted with CeO<sub>2</sub>. *Science of The Total Environment*. 625: 686-695. DOI: <https://doi.org/10.1016/j.scitotenv.2017.12.308>
- [26] Yu, Y., Mottaghi-Tabar, S., Iqbal, M. W., Yu, A., & Simakov, D. S. A. 2021. CO<sub>2</sub> methanation over alumina-supported cobalt oxide and carbide synthesized by reverse microemulsion method. *Catalysis Today*. 379: 250-261. DOI: <https://doi.org/10.1016/j.cattod.2020.08.017>
- [27] Parastaev, A., Hoeben, W. F. L. M., van Heesch, B. E. J. M., Kosinov, N., & Hensen, E. J. M. 2018. Temperature-programmed plasma surface reaction: An approach to determine plasma-catalytic performance. *Applied Catalysis B: Environmental*. 239: 168-177. DOI: <https://doi.org/10.1016/j.apcatb.2018.08.011>